

# Neural Cross-Frequency Coupling Functions in Sleep

Dragana Manasova<sup>1,2</sup> and Tomislav Stankovski<sup>3,4\*</sup>

<sup>1</sup>*Sorbonne Université, Institut du Cerveau–Paris Brain Institute–ICM, Inserm, CNRS, APHP, Hôpital de la Pitié Salpêtrière, Paris, France*

<sup>2</sup>*Université Paris Cité, Paris, France*

<sup>3</sup>*Faculty of Medicine, Ss Cyril and Methodius University, Skopje 1000, North Macedonia*

<sup>4</sup>*Department of Physics, Lancaster University, Lancaster LA1 4YB, United Kingdom*

---

## Abstract

The human brain presents a heavily connected complex system. From a relatively fixed anatomy, it can enable a vast repertoire of functions. One important brain function is the process of natural sleep, which alters consciousness and voluntary muscle activity. On neural level, these alterations are accompanied by changes of the brain connectivity. In order to reveal the changes of connectivity associated with sleep, we present a methodological framework for reconstruction and assessment of functional interaction mechanisms. By analyzing EEG (electroencephalogram) recordings from human whole night sleep, first, we applied a time-frequency wavelet transform to study the existence and strength of brainwave oscillations. Then we applied a dynamical Bayesian inference on the phase dynamics in the presence of noise. With this method we reconstructed the cross-frequency coupling functions, which revealed the mechanism of how the interactions occur and manifest. We focus our analysis on the delta-alpha coupling function and observe how this cross-frequency coupling changes during the different sleep stages. The results demonstrated that the delta-alpha coupling function was increasing gradually from Awake to NREM3 (non-rapid eye movement), but only during NREM2 and NREM3 deep sleep it was significant in respect of surrogate data testing. The analysis on the spatially distributed connections showed that this significance is strong only for within the single electrode region and in the front-to-back direction. The presented methodological framework is for the whole-night sleep recordings, but it also carries general implications for other global neural states.

*Keywords:* Coupling function, Cross-frequency coupling, Bayesian inference, EEG, brainwaves, Sleep  
*Highlights:*

- Delta-alpha coupling functions from EEG (electroencephalogram) of whole night sleep
- Use of dynamical Bayesian inference for phase dynamics from brainwave oscillations
- $\delta$ - $\alpha$  coupling function increased gradually from Awake to NREM3(non-rapid eye movement)
- $\delta$ - $\alpha$  coupling function is significant to surrogates only for NREM2 and NREM3
- Spatially – significance is strong within region and in front-to-back direction

---

\*Corresponding author  
t.stankovski@ukim.edu.mk

## 1. Introduction

Many systems in nature are found to interact, between each other or with the environment, or they have interactions between the subsystems that constitute them [1, 2, 3]. Interactions are particularly important for the brain as a complex system that has many different functions from the same structural connectivity [4]. The interactions of complex dynamical systems can cause gradual or sudden changes in their qualitative dynamics, leading to their grouping, self-organizing, clustering and mutually coordinated synchronization. An important class of such dynamical systems are oscillators, which on the macroscopic scale in the brain can occur as different brainwave oscillations [5].

There exist many powerful methods which study different aspects of the brainwave oscillations and their interactions. Generally in neuroscience, the brain connectivity is classified in three different types. That is, the brain connectivity refers to a pattern of links ("structural, or anatomical, connectivity"), of statistical dependencies ("functional connectivity"), and of causal model interactions ("effective connectivity") between distinct units within a nervous system [6, 7, 8]. The connectivity pattern between the units is formed by structural links such as synapses or fiber pathways, or it represents statistical or causal relationships measured as cross-correlations, coherence, information flow or the all-important coupling function. In this way, therefore, the brain connectivity is crucial to understand how neurons and neural networks process information. A particularly accessible and useful approach has been the study of cross-frequency coupling where one studies connectivity between different brainwave oscillations, usually extracted from an electroencephalograph (EEG) recording [9, 10, 11, 12]. In this work the focus will be on methods for dynamical inference, often also referred to as dynamical filtering or dynamical modeling [13, 14, 15, 16]. In particular such methods involve the analysis of data to reconstruct a dynamical model describing the systems and their interactions. In this way, the dynamical inference methods reconstruct effective connectivity, thus revealing the underlying dynamical mechanisms.

The described dynamical inference methods have been developed and utilized for the reconstruction of coupling functions from data. *Coupling functions* describe how the interaction occurs and manifest, thus revealing a functional mechanism [17]. The design of powerful methods and the explicit assessment of coupling functions has led to applications in different scientific fields including chemistry [18], climate [19], secure communications [20], mechanics [21], social sciences [22], and oscillatory interaction in physiology for cardiorespiratory interactions [23, 24]. Arguably, the greatest recent interest for coupling functions is coming from neuroscience [25]. These works have encompassed the theory and inference of a diversity of neural phenomena, levels, physical regions, and physiological conditions [26, 27, 28, 29, 30, 31, 32, 33]. When the coupling functions describe the interactions between brainwave oscillations with distinctive frequency intervals, then one refers to neural cross-frequency coupling functions [31].

The brain can facilitate various coexisting neural states and functions. Sleep is vitally important state helping to restore the immune, nervous, skeletal, and muscular systems that maintain mood, memory, and cognitive function [34, 35]. Promoted by the internal circadian clock, sleep is a naturally recurring state of the mind and body, characterized by altered consciousness, relatively inhibited sensory activity and reduced muscle activity [36, 37, 38]. Sleep usually occurs as a relatively long overnight process in which the brain goes through several different sleep stages [39, 40, 41, 42, 43]. It is well known that with the onset of sleep, and the different sleep stages, comes also change to the brainwave oscillations [44, 45, 46, 47, 48]. Two of the most pronounced changes appear in the delta and alpha brainwaves. These changes have been followed broadly with different measures of frequency power and statistical dependencies. In our earlier works, we studied neural coupling functions in relation to general anaesthesia [49] and resting state with eyes open and eyes closed [31]. However, up until now, to the best of our knowledge, no one has reconstructed and assessed coupling functions in relation to sleep and its distinctive sleep stages. In this work we present a methodological framework for studying

the delta-to-alpha neural cross-frequency coupling functions from sleep EEG data, and we assess the coupling functions changes associated with the different sleep stages.

## 2. Methods

### 2.1. Sleep recordings

The EEG dataset used in this study comes from the DREAMS database, collected by TCTS laboratory at the University of Mons and the Charleroi Sleep Laboratory at the Université Libre de Bruxelles [50]. It consists of 20 whole night PSG recordings from healthy subjects (16F/4M). The data was collected using a digital 32-channel EEG system (BrainnetTM System of MEDATEC, Brussels, Belgium). In each recording, at least three EEG channels (CZ-A1 or C3-A1, FP1-A1 and O1-A1), two EOG channels (P8-A1, P18-A1) and one submental EMG channel were used. The sampling rate was set to 200 Hz. Each whole night recording was sleep stage scored using both the Rechtschaffen and Kales (R&K) and the American Academy of Sleep Medicine (AASM) protocols. The first annotation was done on 20-second epochs, and the latter on 30-second epochs. Both annotations were produced through a visual inspection by a single expert at the sleep laboratory. In this study, we used the AASM criteria for the sleep stage analyses. For the wavelet analysis and later for the coupling analysis, we grouped the resulting values in respective sleep stages according to the AASM scoring i.e. we separate the wavelet and coupling results from time-intervals of Awake, NREM1 (Non-REM sleep stage), NREM2, NREM3 and REM (Rapid Eye Movement) sleep stage.

### 2.2. Time-frequency wavelet analysis

A comprehensive analysis of neural oscillatory interactions during sleep is given by employing two complementary methods that describe different aspects: the existence and strength of oscillations, and the causal interaction mechanisms.

To calculate the effective neural cross-frequency coupling we first observed the neural oscillations i.e.

the brainwaves during different sleep cycles. This was achieved when the EEG measurements were analysed by continuous wavelet transform (WT) [51, 52]. It is a time-frequency representation containing both the phase and the amplitude dynamics of the oscillatory elements from the analyzed signal.

The continuous wavelet transform of a EEG signal  $x(t)$  is given with the equation:

$$WT(\omega, t) = \int_0^\infty \psi(\omega(u-t))x(u)\omega du. \quad (1)$$

Here,  $\omega$  denotes the angular frequency,  $t$  is the time, and

$$\psi(u) = \frac{1}{2\pi} (e^{i2\pi f_0 u} - e^{\frac{(2\pi f_0)^2}{2}}) e^{-\frac{u^2}{2}}$$

is the complex Morlet wavelet, with central frequency  $f_0 = 1$ ,  $\int \psi(t)dt = 0$ , and with  $i$  being the imaginary unit.

After normalizing (1),  $|W_s(t, f)|^2$  represents an instantaneous estimate of the power spectrum at each time  $t$ , and is referred to as the wavelet power. It is similar to the Fourier transform power spectrum, but by using adaptive windows it achieves logarithmic frequency resolution and high frequency and time localization, allowing for a suitable representation of the spectral structure at the observed frequencies. The brainwave boundaries of the intervals extracted from the EEG signal were  $\delta = 0.8 - 4Hz$ ,  $\theta = 4 - 7.5Hz$ ,  $\alpha = 7.5 - 14Hz$ ,  $\beta = 14 - 22Hz$  and  $\gamma = 22 - 100Hz$ . In this way, by using the wavelet transform we explore the existence of brainwave oscillations in different sleep cycles, and their respective strengths.

### 2.3. Neural coupling functions

The brain is a highly-connected complex system [4], whose interactions can be studied at different levels, many of them carrying important implications for characteristic neural states and diseases. Coupling functions are especially appealing for studying the neural interactions as they can characterize the particular neural mechanisms behind these connections [25, 17, 31]. Not surprisingly, recently, there has been quite a lot of interest for coupling functions in neuroscience.

We start by studying interacting dynamical systems as a system setup, with the focus on coupled oscillators. Then, *coupling functions* describe the physical rule specifying how the interactions occur and manifest. Because they are directly connected with the functional dependencies, coupling functions focus not only on if the interactions exist, but more on how they appear and develop. For example, when studying phase dynamics of coupled oscillators the magnitude of the phase coupling function affects directly the oscillatory frequency and will describe how the oscillations are being accelerated or decelerated by the influence of the other oscillator.

### 2.3.1. Phase dynamics model of interacting oscillations

We model the entire system of neural interactions as a network of pairwise coupled phase oscillators [2]. This oscillator network is defined as:

$$\dot{\phi}_i(t) = \omega_i(t) + q_i(\phi_1, \phi_2, t) + \xi_i(t), \quad (2)$$

where  $i = 1, 2$  is the oscillator index,  $\xi_i$  is the Gaussian white noise, and  $\dot{\phi}_i$  is the instantaneous frequency of each oscillator which is determined by its natural frequency  $\omega_i$  and by a *coupling function* [17]  $q_i$  of the phases  $\phi_{1,2}$  of the two oscillators. The functions  $q_i$  represent the underlying coupling dynamics of the pairwise interaction within the network. Due to the oscillatory nature of the systems, the deterministic section of (2) can be expanded with a second order Fourier expansion into a sum of base functions  $\Phi_k$ , i.e. a series of *sin* and *cos* functions on the full  $(\phi_1, \phi_2)$  argument space, scaled by parameters  $c_k^{(i)}$ :

$$\dot{\phi}_i(t) = \sum_{k=-2}^2 c_k^{(i)} \Phi_k(\phi_1, \phi_2, t) + \xi_i(t). \quad (3)$$

Therefore, the main aim will be to infer this model of coupled phase oscillators, i.e. to infer the parameters of the model base functions  $\Phi_k$  and the noise parameters.

### 2.4. Dynamical Bayesian Inference

To perform the model inference we applied dynamical Bayesian inference [53, 54, 55]. The method reconstructs the matrix of parameters  $\mathcal{M} = \{c_k^{(i)}, D\}$ , which consists of the coupling parameters  $c_k^{(i)}$  and the noise strength  $D$ , thus completely describing the oscillator coupling. We achieve this by utilizing the essence of Bayes' theorem for obtaining the posterior probability density  $p_{\mathcal{X}}(\mathcal{M}|\mathcal{X})$  of the unknown parameters  $\mathcal{M}$  given the data  $\mathcal{X}$  and given the prior probability density  $p_{\text{prior}}(\mathcal{M})$  of the parameters:

$$p_{\mathcal{X}}(\mathcal{M}|\mathcal{X}) = \frac{\ell(\mathcal{X}|\mathcal{M})p_{\text{prior}}(\mathcal{M})}{\int \ell(\mathcal{X}|\mathcal{M})p_{\text{prior}}(\mathcal{M})d\mathcal{M}}. \quad (4)$$

Here, the likelihood function  $\ell(\mathcal{X}|\mathcal{M})$  is obtained through the stochastic integral of the noise term over time, thus leading to the minus log-likelihood function  $S = -\ln \ell(\mathcal{X}|\mathcal{M})$  defined as:

$$S = \frac{L}{2} \ln |D| + \frac{h}{2} \sum_{l=0}^{L-1} (\mathbf{c}_k \frac{\partial \Phi_k(\phi_{\cdot,l})}{\partial \phi} + [\dot{\phi}_l - \mathbf{c}_k \Phi_k(\phi_{*.,l})]^T (\mathbf{D}^{-1}) [\dot{\phi}_l - \mathbf{c}_k \Phi_k(\phi_{*.,l})]), \quad (5)$$

where  $h$  is the sampling time,  $L$  is the length of the time series, and the summation over  $k$  is implicit.

We assume that the prior probability of parameters  $\mathcal{M}$  is a multivariate normal distribution. Then, taking into account the fact that the log-likelihood (5) is of quadratic form, the posterior probability will also be a multivariate normal distribution. The distribution for the parameter vector  $\mathbf{c}$ , its mean  $\bar{\mathbf{c}}$ , and covariance matrix  $\Sigma_{\text{prior}} \equiv \Xi_{\text{prior}}^{-1}$  are then used to recursively obtain the stationary point of  $S$  using:

$$\begin{aligned} \mathbf{D} &= \frac{h}{L} \left( \dot{\phi}_l - \mathbf{c}_k \Phi_k(\phi_{*.,l}) \right)^T \left( \dot{\phi}_l - \mathbf{c}_k \Phi_k(\phi_{*.,l}) \right), \\ \mathbf{c}_k &= (\Xi_{\text{prior}}^{-1})_{kw} \mathbf{r}_w, \\ \mathbf{r}_w &= (\Xi_{\text{prior}})_{kw} \mathbf{c}_w + h \Phi_k(\phi_{*.,l}) (\mathbf{D}^{-1}) \dot{\phi}_l + \\ &\quad - \frac{h}{2} \frac{\partial \Phi_k(\phi_{\cdot,l})}{\partial \phi}, \\ \Xi_{kw} &= (\Xi_{\text{prior}})_{kw} + h \Phi_k(\phi_{*.,l}) (\mathbf{D}^{-1}) \Phi_w(\phi_{*.,l}), \end{aligned} \quad (6)$$

where the summations over  $l = 1, \dots, L$  and over the repeated indices  $k$  and  $w$  are implicit. Finally, the coupling strength of the coupling from oscillator 1 to oscillator 2 is the Euclidean norm of the aforementioned parameters inferred from the phase dynamics:

$$\sigma_{1,2} = \sqrt{\sum_{k=-2}^2 (c_k^{(1,2)})^2}.$$

The neural input data for the inference described here comes in a form of instantaneous phase signals. In practice, the brainwave oscillations are filtered-out from the EEG signals by standard Butterworth filter followed by filtfilt procedure to ensure zero-lag disturbances. From such filtered oscillation signals, we then obtained the protophase by using the Hilbert transformation, after which we applied the protophase-to-phase univariate transformation [21] to obtain the phase signals that act as input to the Bayesian inference.

### 2.5. Statistical analysis and Surrogate time-series testing

Even for unrelated or uncoupled oscillations, the coupling between the signals is generally positive, however small. This is the reason why a significance threshold must be defined, above which the coupling will be considered significant and indicative of genuine connectivity and interdependence. That threshold is defined by constructing randomized surrogates [56, 57] of the original signals and calculating the coupling functions for these surrogates as well. The obtained results serve as a baseline reference in order to confirm the relative statistical significance of the coupling of the original signals. We used a surrogate threshold of mean plus two standard deviations of the coupling calculated from the surrogates, and for generating the surrogate time series we used the cycle phase permutation (CPP) surrogates [57]. Cycle phase permutation surrogates are designed for phase dynamics. These surrogates are constructed to test the interdependence between systems and are generated by rearranging the cycles within the extracted phase. If the phase dynamics of two systems are not independent, then phase evolution over time of one system will be dependent on the phase evolution of the other system. Rearranging the cycles by random permutation destroys this dependence, whilst

preserving the general form of the phase dynamics of each system [57]. More technical details about the procedure of CPP surrogate testing can also be found in the Supplementary Material.

For calculating the statistical difference between coupling distributions, we use the standard Wilcoxon statistical test, where  $p < 0.05$  was considered as significant. The different coupling distributions did not form a statistical family and multiple comparison test were not needed. For visually presenting the statistical differences we use the standard boxplot, which refer to the descriptive statistics (median, quartiles, maximum and minimum).

## 3. Results

This section shows comprehensive analysis of the oscillations and their interactions. We begin by looking into the presence and extent of the brainwave oscillations by conducting a wavelet analysis. We then reconstruct the delta-alpha coupling functions and quantify their coupling strength in relation to the different sleep stages.

### 3.1. Existence and strength of brainwave oscillations

In order to observe the strength of different oscillations, we used the wavelet transform (WT) analysis [58, 59]. Fig. 1 **A** shows an EEG signal from a subject during one night sleep for the O1 electrode, which acts as an input signal for the wavelet analysis. The time-frequency wavelet transform (Fig. 1 **B**) presents the detailed frequency and time changes throughout the night sleep. Fig. 1 **C** then shows the time-averaged frequency-only wavelet transform, where the specific delta and alpha brainwave oscillation can be observed. [The analysis of all the brainwave oscillations are given in Supplementary Material.] The three plots Fig. 1 **A**, **B** and **C** are aligned in time (**A** and **B**) and frequency (**B** and **C**) for comparison. These results show that there are well pronounced delta  $\delta$  and alpha  $\alpha$  brainwave oscillations (Fig. 1 **C**) and that this frequency power varies and goes through transitions over the course of time during the sleep (Fig. 1 **A**).

Having seen the time-frequency wavelet representation from a single representative subject (Fig. 1 **A**,

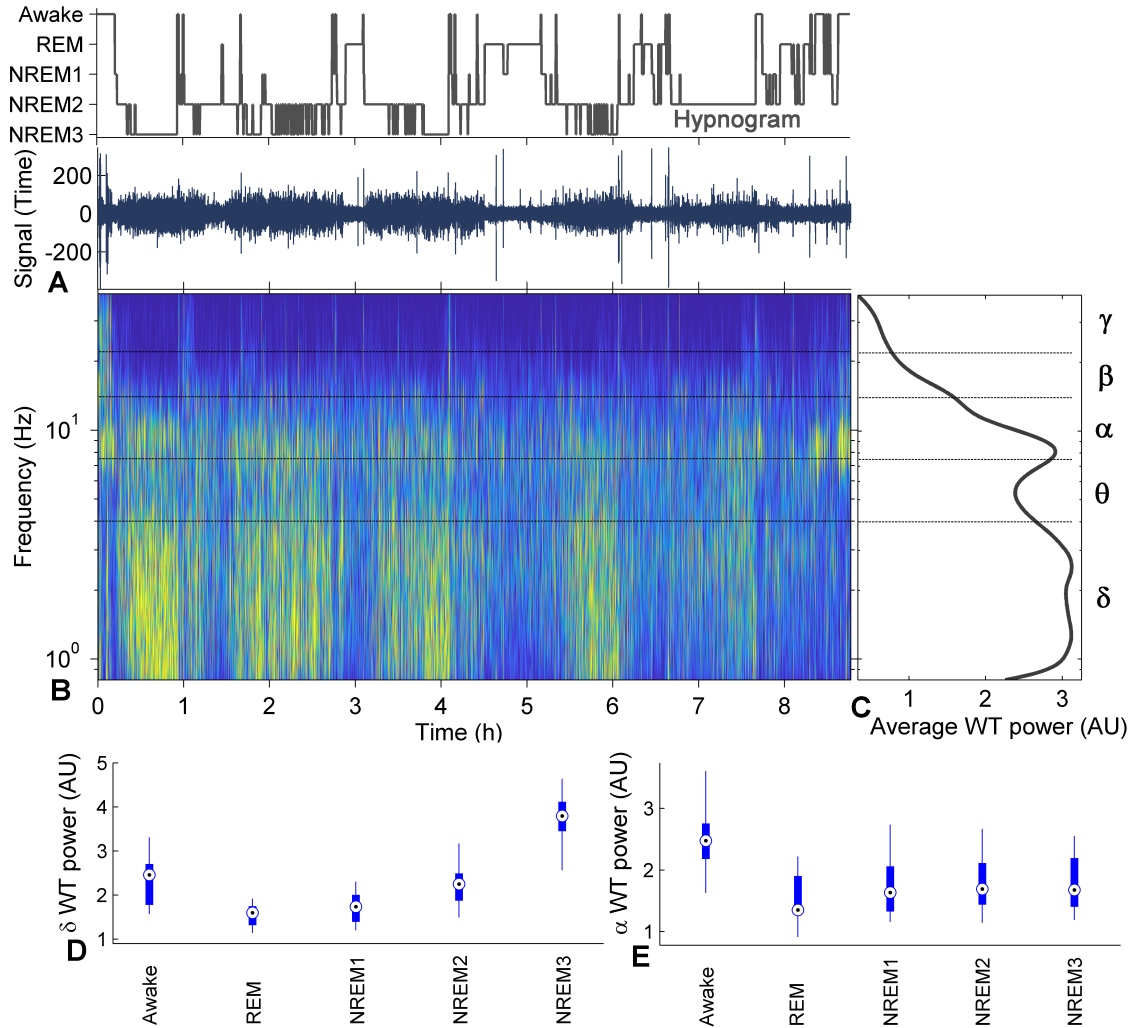


Figure 1: **The brainwave oscillations during sleep – Wavelet transform analysis.** The top panel shows the Hypnogram with the accompanied sleep staging. **A** shows a sample EEG time-series, **B** shows a time-frequency wavelet transform and **C** shows the time-averaged spectral frequency content. **A**, **B** and **C** are the time, time-frequency and frequency representation, respectively, of a same sample Cz electrode EEG recording from a subject during one night sleep. The dashed lines indicate the five brainwave oscillation intervals  $\delta$ ,  $\theta$ ,  $\alpha$ ,  $\beta$  and  $\gamma$  as indicated on the right axes on **C**. The boxplots on **D** show the average power in  $\delta$  interval for all subjects of the O1 EEG electrode, for the five stages of sleep. Similarly, the boxplots on **E** show the average power in  $\alpha$  interval for all subjects of the same O1 electrode. AU stands for arbitrary units.

**B** and **C**), we now move to wavelet analysis on group of subjects (Fig. 1 **D** and **E**). The wavelet power of the delta  $\delta$  brainwave oscillation varies between different sleep stages (Fig. 1 **D**). Namely, the power in the Awake state is significantly reduced in the REM

sleep stage, which then gradually increases through NREM1, NREM2 and NREM3. Here, one should note that the  $\delta$  power in NREM3 is the highest, even higher than the Awake stage. The wavelet power of the alpha  $\alpha$  brainwave oscillation is highest for the

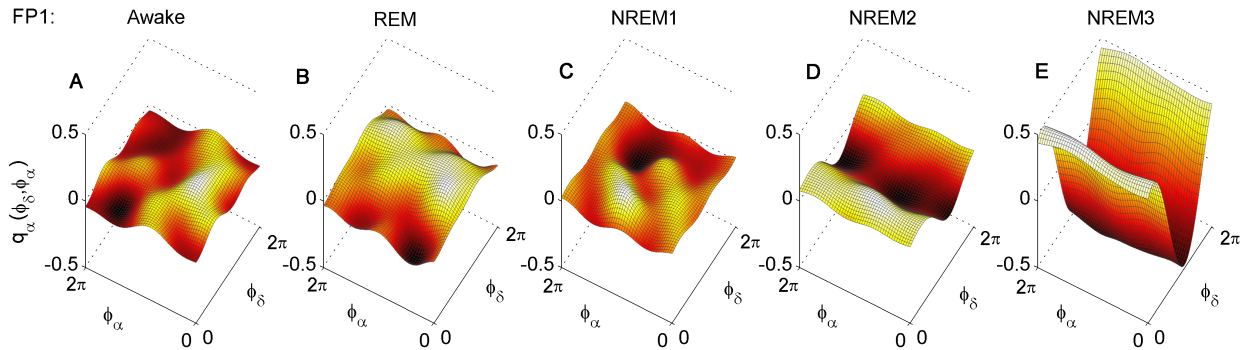


Figure 2: **The  $\delta$ -to- $\alpha$  neural coupling functions in sleep.** A to E present the group average  $\delta$ -to- $\alpha$  coupling functions for the five different states in the sleep cycle, for the Fp1 EEG electrode. Note that for comparison the scale on all the z-axis for the coupling function amplitude are the same.

Awake stage, after which there is significant decrease for the sleep stages (Fig. 1 D). Here REM is slightly lower than the other three NREM stages, which are of relatively the same order.

### 3.2. The $\delta$ -to- $\alpha$ neural coupling functions in sleep

Next, we turn our attention to the neural  $\delta$ -to- $\alpha$  cross-frequency coupling functions for the different sleep stages. After applying the dynamical Bayesian inference on the phases from the EEG data, we reconstructed the  $\delta$ -to- $\alpha$  coupling functions – as shown in Fig. 2. Here, the coupling functions are averaged for the different sleep stages. Note that, for comparison between stages the coupling functions are aligned left-to-right from Awake to NREM3.

We see that the coupling function for the Awake stage is very low with varying and not well defined form of the function (Fig. 2 A). The results are qualitatively similar for the coupling functions of REM sleep and the first stage of light sleep NREM1 (Fig. 2 B and C), where again the functional forms are varying and without a well defined form. Then, for the NREM2 and the NREM3 stage, the  $\delta$ -to- $\alpha$  neural coupling functions were significantly increased and the form of the function had characteristic wave shape (Fig. 2 D and E). This change appears to be gradual, where the coupling function in NREM3 had higher amplitude than NREM2, which in turn was higher than the coupling functions in the other three stages.

The form of the  $\delta$ -to- $\alpha$  coupling function for the NREM2 and NREM3 (Fig. 2 D and E) has characteristic wave shape. The wave changes mostly along the  $\phi_\delta$ -axis and less along the  $\phi_\alpha$ -axis. This form thus reveals that the  $\delta$ -to- $\alpha$  coupling function in the dynamics of  $\alpha$  brainwave oscillations  $q_\alpha(\phi_\delta, \phi_\alpha)$  is predominantly dependent on the  $\delta$  dynamics i.e. this is a direct coupling from  $\delta$  [49]. By going back to the phase model Eq. (2), one can notice that the coupling function  $q_\alpha(\phi_\delta, \phi_\alpha)$  is additive to the frequency parameter  $\omega_\alpha$ . Thus, the characteristic wave form reveals the mechanism underlying the phase dynamics interaction: it shows in detail how the  $\alpha$  brainwave oscillations are accelerated or decelerated, as an effect of the direct influence from the  $\delta$  brainwave oscillations. In other words, when looking at the NREM3 coupling function wave, from 0 to  $\pi$  delta phase  $\phi_\delta$ , there is a deceleration of  $\alpha$  oscillations, and from  $\pi$  to  $2\pi$   $\phi_\delta$ , there is an acceleration of alpha oscillations [17]. The coupling functions in Fig. 2 thus show the qualitative nature of the  $\delta$ -to- $\alpha$  interaction in the different sleep stages.

### 3.3. The $\delta$ -to- $\alpha$ coupling strength

To investigate the interactions in a quantitative way, we calculated the  $\delta$ -to- $\alpha$  coupling strength, as a norm from the aforementioned  $\delta$ -to- $\alpha$  coupling functions. The boxplots in Fig. 3 show the coupling strength of the group of subjects, for different sleeping stages. Only the coupling strength for NREM2

	Fp1 $_{\delta\alpha}$	Cz $_{\delta\alpha}$	O1 $_{\delta\alpha}$	Fp1 $_{\delta}$ -Cz $_{\alpha}$	Fp1 $_{\delta}$ -O1 $_{\alpha}$	Cz $_{\delta}$ -Fp1 $_{\alpha}$	Cz $_{\delta}$ -O1 $_{\alpha}$	O1 $_{\delta}$ -Fp1 $_{\alpha}$	O1 $_{\delta}$ -Cz $_{\alpha}$
Awake	2.20	2.18	2.07	2.19	2.08	2.20	2.08	2.19	2.16
REM	2.32	2.35	2.31	2.32	2.29	2.33	2.26	2.33	2.33
NREM1	2.35	2.33	2.29	2.29	2.31	2.32	2.28	2.34	2.37
NREM2	2.42	<b>2.49</b>	<b>2.49</b>	<b>2.50</b>	<b>2.48</b>	2.43	<b>2.47</b>	2.40	<b>2.52</b>
NREM3	<b>2.48</b>	<b>2.56</b>	<b>2.50</b>	<b>2.54</b>	<b>2.51</b>	2.39	<b>2.52</b>	2.40	2.49
Surrog.	2.45	2.48	2.47	2.50	2.47	2.44	2.47	2.44	2.49

Table 1: Median values for the coupling strength  $\varepsilon_{\delta-\alpha}$  for the five states of the sleep cycle and for the all the coupling relationships investigated. Note that the first three coupling relationships are from a single electrode, while the other six couplings are from mixed electrodes for spatial investigation. Coupling strengths that were statistically significant in respect of the surrogates are presented with bold text. Surrogate thresholds, calculated as mean plus two standard deviations, are shown with grey in the last row. The values are cut to two decimal places for succinct presentation, we note however, that the significance of the NREM2 for Fp1 $_{\delta}$ -Cz $_{\alpha}$  is because the coupling  $\varepsilon_{\delta-\alpha} = 2.5051$  is larger than its surrogate threshold  $surr = 2.5005$ .

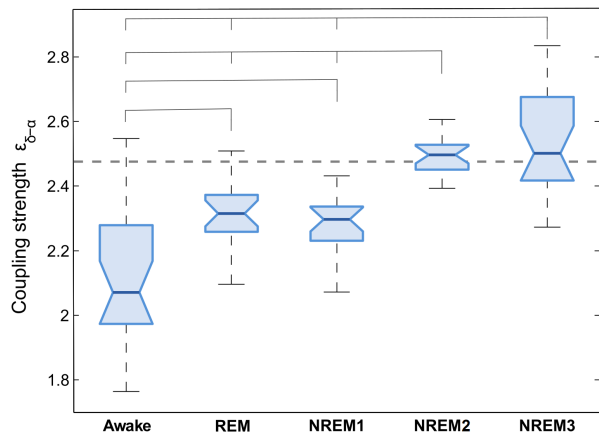


Figure 3: **Average  $\delta$ - $\alpha$  coupling strength.** The boxplots show the average coupling strength  $\varepsilon_{\delta-\alpha}$  for the group subjects for the O1 electrode, presented individually for each state of the sleep cycle. The dashed line represents the surrogate data threshold. The connecting lines on the top, from left to right, represent if two boxplots distributions are statistically and significantly different ( $p < 0.05$ ).

and NREM3 sleep stages were significant in respect to the surrogate threshold (indicated by dashed line in Fig. 3). (This quantitative result is consistent with the coupling function observations for NREM2 and NREM3 in Fig. 2.) There were also differences between the boxplots for the sleep stages. Here one can observe three groups: i) Awake, ii) REM and

NREM1, and iii) NREM2 and NREM3. Namely, the coupling for the Awake stage was lowest and significantly different from all the other four sleep stages. REM and NREM1 stages were similar and they were both significantly greater than Awake, while smaller than NREM2 and NREM3. The coupling during NREM2 and NREM3 was similar between them and significantly greater than the other three sleep stages. The overall trend from comparison of all the five stages is that there is gradual increase of the coupling strength when going from Awake to NREM3. Quantitative statistical analysis with linear regression for the gradual increase is given in the Supplementary Material.

The previous observation of coupling strength (Fig. 3) was only from one EEG channel. Next, we extend this to three channels (prefrontal Fp1, center Cz and occipital O1), in order to assess also the spatial distribution of the interactions. We present these results tabularly in Tab. (1). Here, we present two groups of results: i) between delta and alpha brainwaves within the same channel location, and ii) spatially distant delta and alpha i.e. combinations with delta from one channel and alpha brainwave from other channel. First, we observe the three columns at the beginning of the table for Fp1 $_{\delta\alpha}$ , Cz $_{\delta\alpha}$  and O1 $_{\delta\alpha}$ . Here, there is increase of the coupling strength when going from Awake to NREM3, where NREM2 and NREM3 are significant in respect of surrogates (with bold text).

An exception is only  $Fp1_{\delta\alpha}$  where only NREM3 had significant coupling with respect to surrogates.

The second group of spatially distant interactions shows interesting trend – there is a strong and significant coupling from links going in front-to-back direction, but much lower and not-significant when going in back-to-front direction. Namely, in the  $Fp1_{\delta}-Cz_{\alpha}$ ,  $Fp1_{\delta}-O1_{\alpha}$  and  $Cz_{\delta}-O1_{\alpha}$  connections where the information flow is from front to back of the head, there is strong coupling strength with NREM2 and NREM3 significant to surrogates in all three connections. Contrary to this, in the back-to-front direction of information flow the links  $Cz_{\delta}-Fp1_{\alpha}$ ,  $O1_{\delta}-Fp1_{\alpha}$  and  $O1_{\delta}-Cz_{\alpha}$  had low coupling strength, and they were not significant to surrogates (exception is only NREM2 for  $O1_{\delta}-Cz_{\alpha}$ ). Overall, the coupling strength from Awake to NREM3 gradually increased for all interaction combinations, though the significance with respect to surrogates is strong only for within the region and in the front-to-back direction.

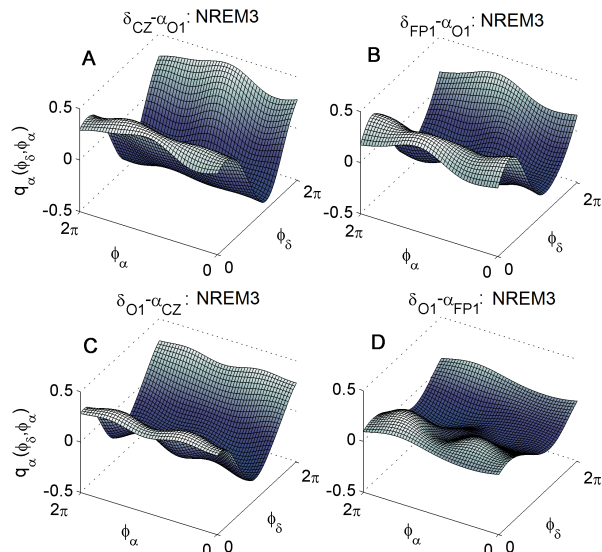


Figure 4: **The spatial  $\delta$ -to- $\alpha$  neural coupling functions in sleep.** All four  $\delta$ -to- $\alpha$  coupling functions are for the NREM3 stage sleep, but the  $\delta$  and  $\alpha$  oscillations are coming from different spatial EEG electrodes. They are subject group averages. For the coupling function in **A** the  $\delta$  is from the Cz electrode, while  $\alpha$  is from the O1 electrode; for **B**  $\delta$  is from Fp1 and  $\alpha$  is from O1 electrode; for **C**  $\delta$  is from O1 and  $\alpha$  is from Cz electrode; and for **D**  $\delta$  is from O1 and  $\alpha$  is from Fp1 electrode.

### 3.4. The spatially distant coupling functions

Next, we analyzed the  $\delta$ -to- $\alpha$  coupling functions from spatially distant links where the  $\delta$  brainwave comes from one, and the  $\alpha$  brainwave comes from other EEG channel. Fig. 4 presents four examples of such spatial  $\delta$ -to- $\alpha$  coupling functions for the NREM3 sleep stage which had highest coupling strength. Fig. 4 A and B for the coupling functions of the front-to-back  $\delta_{Cz}-\alpha_{O1}$  and  $\delta_{Fp1}-\alpha_{O1}$ , respectively, demonstrate the same form of coupling function as Fig. 2, at the same time having relatively high amplitude i.e. coupling strength. The other two coupling functions in Fig. 4 C and D for the back-to-front (opposite direction from A and B) had much lower amplitude and coupling strength. Nevertheless, the form of the coupling function in C and D is qualitatively similar to the form in A and B. These reinstates that the NREM3 coupling functions are the strongest and most prominent among the sleep stages, both in strength and functional form.

### 3.5. The analogy and relation to sleep spindles

The main focus in this study is on the delta ( $\delta = 0.8 - 4Hz$ ) and alpha ( $\alpha = 7.5 - 14Hz$ ) brain-wave oscillations and how they interact, seen through their phase dynamics. On the other hand, a lot of works about EEG dynamics and sleep have studied the interactions of slow waves ( $< 4Hz$ ) and spindles ( $11 - 16Hz$ ). As the alpha band we analyzed and the sleep spindles band (sigma  $\sigma$ ) largely overlap on the frequency spectrum, the question if the observed interaction reflects the interaction from delta to one or the other band, and how they relate to the different sleep stages, naturally arises. To understand this, we have performed separate analyses, methodologically as before, but now for the interaction of: (i) delta to alpha ( $\alpha' = 8 - 12Hz$ ) and (ii) delta to spindles sigma ( $\sigma = 12 - 16Hz$ ). [Note that we called the new band  $\alpha'$  as it is slightly different frequency interval from the initially used  $\alpha$ .]

We note also, that there are many sleep studies which separate the spindles into two parts – slow spindles ( $\sigma_1 = 9 - 12Hz$ ) and fast spindles ( $\sigma_2 = 12 - 15Hz$ ) and then they study how the two interact with slow waves [60, 61, 62, 63]. In this sense,

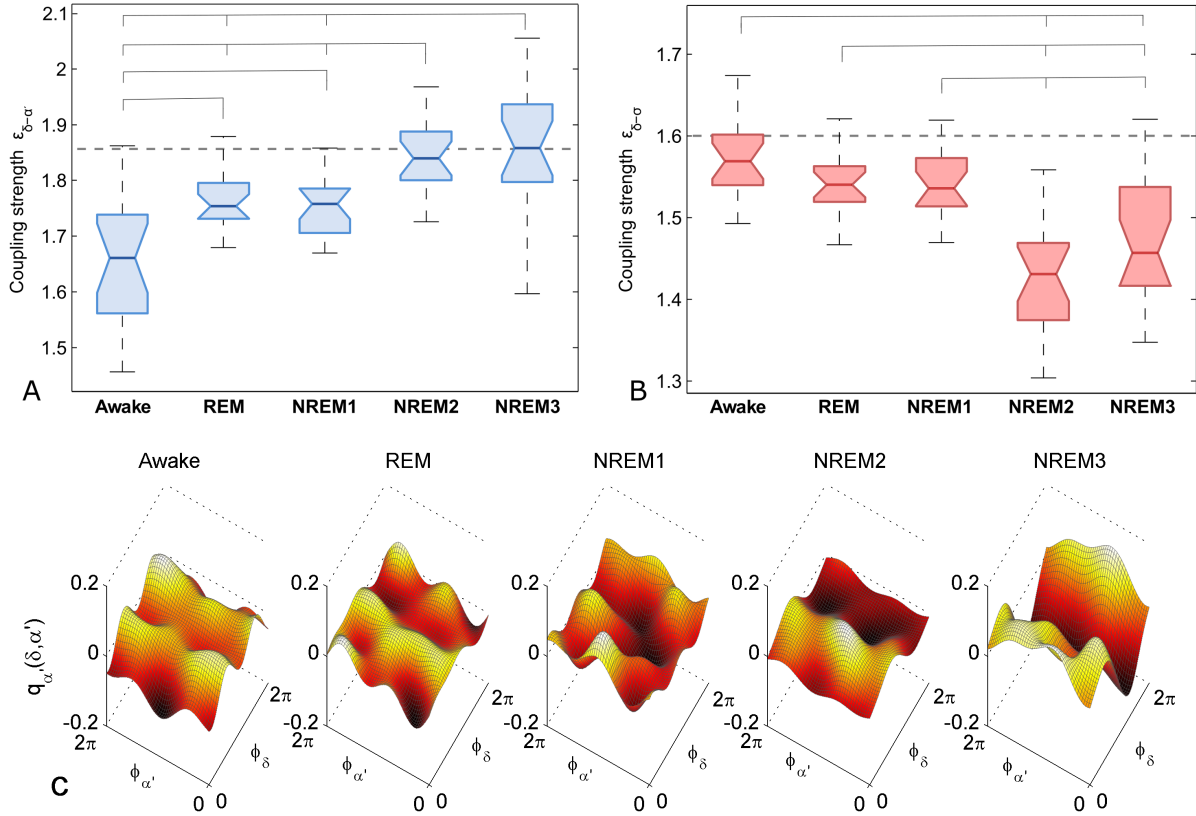


Figure 5: **The  $\delta$ -to- $\alpha'$  and the  $\delta$ -to- $\sigma$  neural coupling in sleep.** Average  $\delta$ - $\alpha'$  **A** and  $\delta$ - $\sigma$  **B** coupling strength for the group subjects for the O1 electrode, presented individually for each state of the sleep cycle. The dashed line represents the surrogate data threshold. The connecting lines on the top, from left to right, represent if two boxplots distributions are statistically and significantly different ( $p < 0.05$ ). **C** present the group average  $\delta$ - $\alpha'$  coupling functions for the five different states in the sleep cycle, for the Fp1 EEG electrode.

what we are doing here with the separation to alpha and sigma, amounts to a similar approach as the separation to slow and fast spindles.

The analysis about the  $\delta$ -to- $\alpha'$  and the  $\delta$ -to- $\sigma$  coupling is presented in Fig. 5. The coupling strength quantitative and statistical analysis (similar to those in Fig. 3) for the  $\delta$ -to- $\alpha'$  interaction Fig. 5 **A** shows a similar picture as seen before – that there is a gradually increasing coupling from Awake to NREM3, with some portion being significant in respect of surrogates (cf. NREM2 and NREM3) and with statistical differences between the different sleep stages. The coupling strength for the other  $\delta$ -to- $\sigma$  interaction Fig. 5

**B** shows much lower coupling and not significant in respect of surrogates. The  $\delta$ -to- $\alpha'$  coupling functions Fig. 5 **C**, where there were some significant couplings, show a more varying form of functions, but qualitatively similar form as the one observed before in Fig. 2, especially for the NREM2 and NREM3 sleep stages. In summary of the separate  $\alpha'$  and  $\sigma$  phase dynamics analysis, we have seen that the observed interaction is predominantly on account of the  $\delta$ -to- $\alpha'$  coupling, and it is low and not significant for the  $\delta$ -to- $\sigma$  coupling.

## 4. Discussion

In summary, we have analyzed sleep effects on the neural oscillatory dynamics and interactions. We presented a methodological framework for analyzing the oscillations and their interaction mechanisms. The framework is quite comprehensive in a sense that it encompasses a wavelet transform describing the existence and strength of the oscillations, followed by a detailed dynamical Bayesian inference of the phase dynamics and the underlying coupling functions which reveal in detail the interaction mechanisms. This methodology probed directly into the dynamics of the neural oscillations and the mechanisms of how they affect causally each other to accelerate or decelerate their oscillations. The analysis were able to follow the time-evolving dynamics in order to trace the transitions due to different sleep stages. Because of this, we were able to group and average the time-intervals of the analysis within the specific sleep stages. In this way, we identified a specific form of the delta-to-alpha coupling function during the sleep stages. The quantitative results showed number of significant changes due to the different nature of the sleep epochs.

It is well known that delta and alpha brainwave oscillations play an important role in the brain dynamics [45, 46, 35, 47, 48]. For instance, there are differences in frequency and power during different sleep stages which appear in the separate delta and alpha brainwave dynamics [64, 65, 66, 67] and in their related alpha-delta effect [68, 69]. Thus studying the delta-alpha cross-frequency coupling, can bring important insight in the neural mechanisms of sleep. For example, in a previous study about general anesthesia [49] all the different brainwave coupling combinations were investigated and only those that were statistically significant to surrogate data testing were studied in detail – here the delta-alpha was one of the most significant and pronounced interaction. Similarly, previous works observe a prominent delta-alpha coupling in resting state [11], during the orienting response [70], and during sleep within the network physiology approach [47]. Therefore, the choice to investigate the delta-to-alpha coupling had a direct relevance for the present study of the nature of sleep,

where the use of coupling functions probed into the interaction mechanisms.

Our results demonstrated that there were specific changes in the delta and alpha oscillations and how they interact over the different sleep stages. Integrating the results together, we observed that the changes in the power of delta and alpha oscillations (Fig. 1) were followed by changes in the form of the delta-to-alpha coupling function (Fig. 2) and coupling strength (Fig. 3 and Tab. 1). These interaction changes were increased gradually from Awake to NREM3, for all the interaction combinations. The coupling function and the coupling strength analysis showed that only during NREM2 deep sleep and NREM3 one could observe significant interactions in respect to surrogates. The analysis on the spatially distributed connections (Fig. 4 and Tab. 1) showed that this significance is strong only for within the single electrode region and in the front-to-back direction. This is consistent with a previous study [71], where using a directed transfer function (DFT) analysis before and after sleep onset, the authors observed a directed antero-posterior functional coupling post sleep-onset. This information flow was opposite to their observation in pre-sleep onset EEG activity, where a posterior-to frontal propagation of activity was found. Similarly, another study [72] reported differences in the prevalence of slow oscillations across regions. Namely, higher slow oscillations density in anterior and central electrodes compared to temporal and posterior areas.

In our study, the delta band captures cortically-driven slow oscillations of large amplitudes. Whereas the alpha band also encompasses sleep spindles which are thalamically-driven oscillatory activity. Spindles and spindle/slow oscillations complexes are shown to be tightly coupled in NREM2 sleep using a modulation index analysis [73]. To study cross-frequency coupling another study employed a debiased phase-amplitude coupling z-scored (dPACz) analysis [72]. They reported a stronger coupling of slow-oscillations and fast spindles (12.5 - 15 Hz) in NREM2 and the reverse for slow spindles (9 - 12.5 Hz), with the coupling of slow oscillations and spindles being the highest in NREM3 for fast spindles. The observed deceleration and acceleration of alpha  $\alpha$  and alpha prime  $\alpha'$

along the delta phases during NREM3 (and somewhat NREM2) – Fig. 2 and Fig. 5 C, could be analogous to the reported increases in slow spindles in the first part of the slow waves, and a decrease in fast spindles in the ascending part of the slow wave [61].

The specific form of the delta-to-alpha coupling function (Fig. 2 and Fig. 4) showed that this is a predominantly direct influence from delta to alpha, and demonstrated in detail how and when the alpha oscillations are accelerated and decelerated due to the causal influence from the delta oscillations. It is important to note that, this form of the coupling function is qualitatively similar to the delta-to-alpha coupling functions observed in our previous studies in relation to general anesthesia [49] and resting state [31]. Namely, the delta-to-alpha coupling function in the generalized deep anesthesia induced by propofol and sevoflurane anesthetics was significantly greater than in awake state [49] and it was similar in the form as the one we showed here with sleep. Similarly, the eyes-closed resting state had higher delta-to-alpha coupling function than the eyes-opened resting state [31], and it was of similar form as the one we observed here for sleep, though the resting awake state had much lower and more varying form of the coupling function. Importantly, the current result about sleep stages showed that the delta-to-alpha coupling function increases gradually from awake to deep sleep in NREM3 stage. In fact, the delta-to-alpha coupling function was most similar between the generalized deep anesthesia and the NREM3 deep sleep stage. This points towards some commonality of reduced arousal and awareness in these global states, thus adding to the discussion about the differences and similarity of sleep stages and anesthesia phases, specifically the EEG signal in NREM3 sleep being similar to that of the phase 2 anesthesia [74, 75, 76].

Finally, it is worth noting that we presented the methodological framework for the whole-night sleep recordings, however, the framework carries important implications and can readily be used also for other forms of sleep recordings, or other neural states more generally.

## References

- [1] A. T. Winfree, Biological rhythms and the behavior of populations of coupled oscillators, *J. Theor. Biol.* 16 (1) (1967) 15.
- [2] Y. Kuramoto, *Chemical Oscillations, Waves, and Turbulence*, Springer-Verlag, Berlin, 1984.
- [3] A. Pikovsky, M. Rosenblum, J. Kurths, *Synchronization – A Universal Concept in Nonlinear Sciences*, Cambridge University Press, Cambridge, 2001.
- [4] H.-J. Park, K. Friston, Structural and functional brain networks: from connections to cognition, *Science* 342 (6158) (2013) 1238411.
- [5] G. Buzsáki, A. Draguhn, Neuronal oscillations in cortical networks, *Science* 304 (2004) 1926–1929.
- [6] B. Horwitz, The elusive concept of brain connectivity, *Neuroimage* 19 (2) (2003) 466–470.
- [7] K. J. Friston, Functional and effective connectivity: a review, *Brain. Connect.* 1 (1) (2011) 13–36.
- [8] M. Rubinov, O. Sporns, Complex network measures of brain connectivity: uses and interpretations, *Neuroimage* 52 (3) (2010) 1059–1069.
- [9] R. T. Canolty, E. Edwards, S. S. Dalal, M. Soltani, S. S. Nagarajan, H. E. Kirsch, M. S. Berger, N. M. Barbaro, R. T. Knight, High gamma power is phase-locked to theta oscillations in human neocortex, *Science* 313 (5793) (2006) 1626–1628.
- [10] O. Jensen, L. L. Colgin, Cross-frequency coupling between neuronal oscillations, *Trends Cognit. Sci.* 11 (7) (2007) 267–269.
- [11] V. Jirsa, V. Müller, Cross-frequency coupling in real and virtual brain networks, *Frontiers Comput. Neurosci.* 7 (2013) 78.
- [12] P. Sorrentino, M. Ambrosanio, R. Rucco, J. Cabral, L. L. Gollo, M. Breakspear,

- F. Baselice, Detection of cross-frequency coupling between brain areas: An extension of phase linearity measurement, *Frontiers in Neuroscience* 16.
- [13] R. E. Kalman, A new approach to linear filtering and prediction problems, *J. Fluid. Eng.* 82 (1) (1960) 35–45.
- [14] H. U. Voss, J. Timmer, J. Kurths, Nonlinear dynamical system identification from uncertain and indirect measurements, *Int. J. Bifurcat. Chaos* 14 (06) (2004) 1905–1933.
- [15] U. von Toussaint, Bayesian inference in physics, *Rev. Mod. Phys.* 83 (3) (2011) 943–999.
- [16] K. J. Friston, L. Harrison, W. Penny, Dynamic causal modelling, *Neuroimage* 19 (4) (2003) 1273–1302.
- [17] T. Stankovski, T. Pereira, P. V. E. McClintock, A. Stefanovska, Coupling functions: Universal insights into dynamical interaction mechanisms, *Rev. Mod. Phys.* 89 (33) (2017) 045001.
- [18] I. Z. Kiss, C. G. Rusin, H. Kori, J. L. Hudson, Engineering complex dynamical structures: Sequential patterns and desynchronization, *Science* 316 (5833) (2007) 1886–1889.
- [19] W. Moon, J. S. Wettlaufer, Coupling functions in climate, *Phil. Trans. R. Soc. A* 377 (2160) (2019) 20190006.
- [20] T. Stankovski, P. V. E. McClintock, A. Stefanovska, Coupling functions enable secure communications, *Phys. Rev. X* 4 (2014) 011026.
- [21] B. Kralemann, L. Cimponeriu, M. Rosenblum, A. Pikovsky, R. Mrowka, Phase dynamics of coupled oscillators reconstructed from data, *Phys. Rev. E* 77 (6, Part 2) (2008) 066205.
- [22] S. Ranganathan, V. Spaiser, R. P. Mann, D. J. T. Sumpter, Bayesian dynamical systems modelling in the social sciences, *PLoS ONE* 9 (1) (2014) e86468.
- [23] B. Kralemann, M. Frühwirth, A. Pikovsky, M. Rosenblum, T. Kenner, J. Schaefer, M. Moser, In vivo cardiac phase response curve elucidates human respiratory heart rate variability, *Nat. Commun.* 4 (2013) 2418.
- [24] D. Lukarski, D. Stavrov, T. Stankovski, Variability of cardiorespiratory interactions under different breathing patterns, *Biomedical Signal Processing and Control* 71 (2022) 103152.
- [25] T. Stankovski, Coupling functions in neuroscience, in: *Physics of Biological Oscillators*, Springer, 2021, pp. 175–189.
- [26] C. Bick, M. Goodfellow, C. R. Laing, E. A. Martens, Understanding the dynamics of biological and neural oscillator networks through exact mean-field reductions: a review, *Journal of Mathematical Neuroscience* 10 (2020) 9.
- [27] A. Yeldesbay, G. R. Fink, S. Daun, Reconstruction of effective connectivity in the case of asymmetric phase distributions, *J. Neurosci. Methods* 317 (2019) 94–107.
- [28] K. Suzuki, T. Aoyagi, K. Kitano, Bayesian estimation of phase dynamics based on partially sampled spikes generated by realistic model neurons, *Front. Comput. Neurosci.* 11 (2018) 116.
- [29] A. Jafarian, P. Zeidman, V. Litvak, K. Friston, Structure learning in coupled dynamical systems and dynamic causal modelling, *Phil. Trans. R. Soc. A* 377 (2019) 20190048.
- [30] H. Su, C. Huo, B. Wang, W. Li, G. Xu, Q. Liu, Z. Li, Alterations in the coupling functions between cerebral oxyhaemoglobin and arterial blood pressure signals in post-stroke subjects, *PloS One* 13 (4) (2018) e0195936.
- [31] T. Stankovski, V. Ticcinelli, P. V. E. McClintock, A. Stefanovska, Neural cross-frequency coupling functions, *Front. Syst. Neurosci.* 11 (33) (2017) 10.3389/fnsys.2017.00033.
- [32] C. N. Takembo, A. Mvogo, H. P. E. Fouda, T. C. Kofané, Effect of electromagnetic radiation on the dynamics of spatiotemporal patterns

- in memristor-based neuronal network, *Nonlin. Dyn.* (2018) 1–12.
- [33] A. Gruszecka, M. K. Nuckowska, M. Waskow, J. Kot, P. J. Winklewski, W. Guminski, A. F. Frydrychowski, J. Wtorek, A. Bujnowski, P. Lass, et al., Coupling between blood pressure and subarachnoid space width oscillations during slow breathing, *Entropy* 23 (1) (2021) 113.
- [34] M. A. Carskadon, W. C. Dement, et al., Normal human sleep: an overview, *Principles and practice of sleep medicine* 4 (1) (2005) 13–23.
- [35] J. M. Krueger, M. G. Frank, J. P. Wisor, S. Roy, Sleep function: Toward elucidating an enigma, *Sleep medicine reviews* 28 (2016) 46–54.
- [36] T. J. Sejnowski, A. Destexhe, Why do we sleep?, *Brain research* 886 (1-2) (2000) 208–223.
- [37] U. Wagner, S. Gais, H. Haider, J. Born, et al., Sleep inspires insight, *Nature* 427 (6972) (2004) 352–355.
- [38] M. Irwin, Effects of sleep and sleep loss on immunity and cytokines, *Brain, behavior, and immunity* 16 (5) (2002) 503–512.
- [39] A. K. Patel, V. Reddy, J. F. Araujo, Physiology, sleep stages, in: *StatPearls* [Internet], StatPearls Publishing, 2022.
- [40] L. S. Imperatori, J. Cataldi, M. Betta, E. Ricciardi, R. A. Ince, F. Siclari, G. Bernardi, Cross-participant prediction of vigilance stages through the combined use of wpli and wsmi eeg functional connectivity metrics, *Sleep* 44 (5) (2021) zsaa247.
- [41] U. Ermis, K. Krakow, U. Voss, Arousal thresholds during human tonic and phasic rem sleep, *Journal of sleep research* 19 (3) (2010) 400–406.
- [42] R. Acharya, O. Faust, N. Kannathal, T. Chua, S. Laxminarayan, Non-linear analysis of eeg signals at various sleep stages, *Computer methods and programs in biomedicine* 80 (1) (2005) 37–45.
- [43] S. Romero, M. Mananas, S. Clos, S. Gimenez, M. Barbanoj, Reduction of eeg artifacts by ica in different sleep stages, in: *Proceedings of the 25th Annual International Conference of the IEEE Engineering in Medicine and Biology Society (IEEE Cat. No. 03CH37439)*, Vol. 3, IEEE, 2003, pp. 2675–2678.
- [44] J. González, D. Mateos, M. Cavelli, A. Mondino, C. Pascovich, P. Torterolo, N. Rubido, Low frequency oscillations drive eeg’s complexity changes during wakefulness and sleep, *Neuroscience* 494 (2022) 1–11.
- [45] M. K. Delimayanti, B. Purnama, N. G. Nguyen, M. R. Faisal, K. R. Mahmudah, F. Indriani, M. Kubo, K. Satou, Classification of brainwaves for sleep stages by high-dimensional fft features from eeg signals, *Applied Sciences* 10 (5) (2020) 1797.
- [46] M. Gorgoni, S. Scarpelli, F. Reda, L. De Genaro, Sleep eeg oscillations in neurodevelopmental disorders without intellectual disabilities, *Sleep Medicine Reviews* 49 (2020) 101224.
- [47] A. Bashan, R. P. Bartsch, J. W. Kantelhardt, S. Havlin, P. C. Ivanov, Network physiology reveals relations between network topology and physiological function, *Nat. Commun.* 3 (2012) 702.
- [48] T. Penzel, M. Hirshkowitz, J. Harsh, R. D. Chervin, N. Butkov 5, M. Kryger, B. Malow, M. V. Vitiello, M. H. Silber, C. A. Kushida, et al., Digital analysis and technical specifications, *Journal of clinical sleep medicine* 3 (02) (2007) 109–120.
- [49] T. Stankovski, S. Petkoski, J. Raeder, A. F. Smith, P. V. E. McClintock, A. Stefanovska, Alterations in the coupling functions between cortical and cardio-respiratory oscillations due to anaesthesia with propofol and sevoflurane., *Phil. Trans. R. Soc. A* 374 (2067) (2016) 20150186.
- [50] S. Devuyt, The dreams databases and assessment algorithm – doi:10.5281/zenodo.2650142.

- [51] I. Daubechies, J. Lu, H. Wu, Synchrosqueezed wavelet transforms: An empirical mode decomposition-like tool, *Appl. and Comput. Harmon. Anal.* 30 (2) (2011) 243–261.
- [52] D. Iatsenko, P. V. E. McClintock, A. Stefanovska, On the extraction of instantaneous frequencies from ridges in time-frequency representations of signals, *Signal Proc.* 125 (2016) 290–303.
- [53] T. Stankovski, A. Duggento, P. V. E. McClintock, A. Stefanovska, Inference of time-evolving coupled dynamical systems in the presence of noise, *Phys. Rev. Lett.* 109 (2012) 024101.
- [54] V. N. Smelyanskiy, D. G. Luchinsky, A. Stefanovska, P. V. E. McClintock, Inference of a nonlinear stochastic model of the cardiorespiratory interaction, *Phys. Rev. Lett.* 94 (9) (2005) 098101.
- [55] T. Stankovski, A. Duggento, P. V. E. McClintock, A. Stefanovska, A tutorial on time-evolving dynamical Bayesian inference, *Eur. Phys. J. Special Topics* 223 (13) (2014) 2685–2703.
- [56] T. Schreiber, H. Kantz, Predictability of complex dynamical systems, in: *Observing and Predicting Chaotic Signals*, Springer, New York, 2003.
- [57] G. Lancaster, D. Iatsenko, A. Pidde, V. Ticcinelli, A. Stefanovska, Surrogate data for hypothesis testing of physical systems, *Phys. Rep.*
- [58] I. Daubechies, *Ten lectures on wavelets*, SIAM, 1992.
- [59] G. Kaiser, *A Friendly Guide to Wavelets*, Birkhäuser, Boston, 1994.
- [60] M. Mölle, T. O. Bergmann, L. Marshall, J. Born, Fast and slow spindles during the sleep slow oscillation: disparate coalescence and engagement in memory processing, *Sleep* 34 (10) (2011) 1411–1421.
- [61] J. G. Klinzing, M. Mölle, F. Weber, G. Supp, J. F. Hipp, A. K. Engel, J. Born, Spindle activity phase-locked to sleep slow oscillations, *Neuroimage* 134 (2016) 607–616.
- [62] F. Dehnavi, P. C. Koo-Poeggel, M. Ghorbani, L. Marshall, Spontaneous slow oscillation-slow spindle features predict induced overnight memory retention, *Sleep* 44 (10) (2021) zsab127.
- [63] A. Ayoub, D. Aumann, A. Hörschelmann, A. Koučekmanesch, P. Paul, J. Born, L. Marshall, Differential effects on fast and slow spindle activity, and the sleep slow oscillation in humans with carbamazepine and flunarizine to antagonize voltage-dependent  $na^+$  and  $ca^{2+}$  channel activity, *Sleep* 36 (6) (2013) 905–911.
- [64] C. L. Ehlers, D. J. Kupfer, Effects of age on delta and rem sleep parameters, *Electroencephalography and clinical neurophysiology* 72 (2) (1989) 118–125.
- [65] M. S. Keshavan, C. F. Reynolds, J. M. Miewald, D. M. Montrose, J. A. Sweeney, R. C. Vasko, D. J. Kupfer, Delta sleep deficits in schizophrenia: evidence from automated analyses of sleep data, *Archives of general psychiatry* 55 (5) (1998) 443–448.
- [66] R. M. Benca, W. H. Obermeyer, C. L. Larson, B. Yun, I. Dolski, K. D. Kleist, S. M. Weber, R. J. Davidson, Eeg alpha power and alpha power asymmetry in sleep and wakefulness, *Psychophysiology* 36 (4) (1999) 430–436.
- [67] W. Scheuler, D. Stinshoff, S. Kubicki, The alpha-sleep pattern, *Neuropsychobiology* 10 (2-3) (1983) 183–189.
- [68] P. Hauri, D. R. Hawkins, Alpha-delta sleep, *Electroencephalography and clinical Neurophysiology* 34 (3) (1973) 233–237.
- [69] S. Vijayan, E. B. Klerman, G. K. Adler, N. J. Kopell, Thalamic mechanisms underlying alpha-delta sleep with implications for fibromyalgia, *Journal of neurophysiology* 114 (3) (2015) 1923–1930.

- [70] J. R. Isler, P. G. Grieve, D. Czernochowski, R. I. Stark, D. Friedman, Cross-frequency phase coupling of brain rhythms during the orienting response, *Brain research* 1232 (2008) 163–172.
- [71] L. D. Gennaro, F. Vecchio, M. Ferrara, G. Curcio, P. M. Rossini, C. Babiloni, Changes in fronto-posterior functional coupling at sleep onset in humans, *Journal of sleep research* 13 (3) (2004) 209–217.
- [72] R. Cox, D. S. Mylonas, D. S. Manoach, R. Stickgold, Large-scale structure and individual fingerprints of locally coupled sleep oscillations, *Sleep* 41 (12) (2018) 175.
- [73] M. Niknazar, G. P. Krishnan, M. Bazhenov, S. C. Mednick, Coupling of thalamocortical sleep oscillations are important for memory consolidation in humans, *PloS one* 10 (12) (2015) e0144720.
- [74] E. N. Brown, R. Lydic, N. D. Schiff, General anesthesia, sleep, and coma, *New Engl. J. Med.* 363 (27) (2010) 2638–2650.
- [75] S. Vacas, P. Kurien, M. Maze, Sleep and anesthesia: Common mechanisms of action, *Sleep medicine clinics* 8 (1) (2013) 1–9.
- [76] J. Jung, T. Kim, General anesthesia and sleep: like and unlike, *Anesthesia and Pain Medicine* 17 (4) (2022) 343–351.